Analysis of the kinetics of the membrane potential generated by cytochrome *c* oxidase upon single electron injection

D.M. Medvedev [a], E.S. Medvedev [b], A.I. Kotelnikov [b], A.A. Stuchebrukhov [c],*

[a] *Chemistry Division, Argonne National Laboratory, Argonne, IL 60439, USA*
[b] *Institute of Problems of Chemical Physics, Russian Academy of Sciences, 142432 Chernogolovka, Moscow, Russia*
[c] *Department of Chemistry, University of California, Davis, CA 95616, USA*

Abstract

In a recent work from this group (Popovic, D. M.; Stuchebrukhov A. A. FEBS Lett. 2004, 566, 126), a model of proton pumping by cytochrome *c* oxidase (CcO) was proposed. The key element of the model is His291 (bovine notation), a histidine ligand to enzyme's CuB redox center, which plays the role of the pump element. The model assumes that upon electron transfer between heme *a* and the binuclear catalytic center of the enzyme, two sequential proton transfers occur: First, a proton from Glu242 is transferred to an unprotonated His291, then a second proton, after reprotonation of Glu242 from the negative side of the membrane, is transferred to a hydroxyl group in the binuclear center, a water molecule is formed, and the first proton, due to proton–proton repulsion, is expelled from His291 to the positive side of the membrane, resulting in a pumping event. In the process the free energy of water formation (i.e., reduction of oxygen) is transformed into a proton gradient across the membrane. The model possesses specific kinetic features. It assumes, for example, that upon electron transfer the first proton is transferred to the proton-loading site of the pump, His291, and not to the catalytic center of the enzyme. Here, we analyze the kinetic properties of the proposed model, and calculate the time dependence of the membrane potential generated by CcO upon a single electron injection into the enzyme. These data are directly compared with recent experimental measurements of the membrane potential generated by CcO. Specifically, F to O, and O to E transitions will be discussed. Several enzymes from different organisms (bovine, two bacterial enzymes, and several mutants) are compared and discussed in detail. The kinetic description, however, is phenomenological, and does not include explicitly the nature of the groups involved in proton translocation, except in terms of their position depth within the membrane; thus, the kinetic equations developed here are in fact describe a generic model, similar, e.g., to that proposed earlier by Peter Rich (P.R. Rich, Towards an understanding of the chemistry of oxygen reduction and proton translocation in the iron-copper respiratory oxidases. Aust. J. Plant Physiol. 22 (1995) 479–486), and which is based on the idea of displacement of the pumped protons by the chemical ones.
© 2005 Elsevier B.V. All rights reserved.

Keywords: Kinetic; Membrane potential; Cytochrome *c*

1. Introduction

Although the structure of cytochrome *c* oxidase (CcO) has been known for almost a decade now [1–3], the mechanism of its proton pumping [4] remains a subject of intense debate [5–8]. A number of models have been proposed (see, e.g., Refs. [9–17]), however, there is no agreement on major issues, such as where the pump element is located and how it pumps protons. The problem is that the measurement of the kinetics of proton

translocation is a notoriously difficult experimental task. The time-resolved measurement of the membrane potential generated by the enzyme has been one of the most fruitful techniques in the studies of CcO. This paper will discuss the data from several such experiments [17–23] in the framework of one specific model proposed recently [24,25].

The pumping mechanism of Refs. [24,25] is based on the idea of kinetic gating [26]. The key elements of the model, see Fig. 1, are the calculated redox dependent changes of the protonation state of His291 (bovine notation), a CuB ligand, and the two chains of water molecules [27,28] connecting Glu242 both to the catalytic site and to His291 (via PropA and Arg439 groups). Glu242 is an experimentally established proton donor, both for

* Corresponding author.
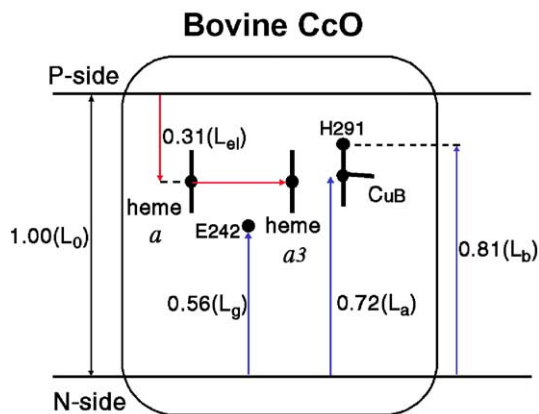 *E-mail address:* stuchebr@chem.ucdavis.edu (A.A. Stuchebrukhov).

Fig. 1. Positions and relative distances of the redox and protonic sites in the enzyme. In the proposed pumping mechanism, an electron transfer between heme a and heme a3/CuB center (BNC) induces two proton transfers: (1) E242 to H291, and then, after reprotonation of E242 from the N-side of the membrane, (2) E242 to BNC. The repulsion between the proton in BNC and that on H291 results in the expulsion of the later to the P-side of the membrane. Distances and corresponding potentials: $L_{el} = V_{el} = 0.31$, $L_a = V_a = 0.72$, $L_b = V_b = 0.81$, $L_0 = V_0 = 1.00$. For bovine enzyme $\beta = 0.5$ [22], and for bacterial enzyme $\beta = 0.75$ [23].

pumping and for chemistry [29–32]. The structure of proton conducting paths suggests that the rate of proton transfer from Glu242 to His291 is likely much faster than that between Glu242 and the hydroxyl group in the catalytic center. The following model therefore was proposed: upon electron transfer between heme *a* and the catalytic center, *two* proton transfers occur sequentially: first, a proton is transferred between Glu242 and His291, then, after re-protonation of Glu242, a second proton is transferred to the binuclear catalytic site, where water is formed. The Coulomb repulsion between the proton residing on His291 and the proton in the catalytic center results in the "expulsion" of the former in the direction of the positive side of the membrane, and eventually giving rise to a pumping event. The energetic feasibility of such proton transfer events has gain further support in a combined DFT/electrostatic calculations of redox dependent pK_a values of Glu242 and His291 [33]. The proton exit path from His291 to the positive side of the membrane and a possible mechanism of preventing the "leaking" of protons from the positive side of the membrane to the negative side through the proton conducting channels of the enzyme were discussed in Ref. [34].

The proposed model has specific kinetic characteristics which give rise to a specific time-dependency of the membrane potential generated by the enzyme when a single electron is transferred to its catalytic site. In this paper, we develop a kinetic description of the pump model, and calculate the time dependence of the membrane potential build up when a single electron is transferred to the binuclear catalytic center of the enzyme, one proton is transferred to the center to form water, and one proton is pumped across the membrane. In this process all charges – an electron and both protons – contribute to the potential build up.

Recently, the measurements of the membrane potential induced by a single electron injection into CcO incorporated into liposome vesicles have been carried out for several

enzymes from different organisms and for different transitions of the catalytic cycle of the enzyme [17–23]. In the absence of direct observation of proton transfer reactions and the groups involved in proton transfer, this type of measurements is one of the most detailed and direct diagnostics of the performance of the enzyme. In this paper, we compare the predicted kinetics of the generated membrane potential with that measured in the experiment and evaluate the feasibility of the proposed His291 model. Specifically F to O and O to E transitions will be discussed. Several enzymes from different organisms (bovine, two bacterial enzymes, and several mutants) are compared and discussed in detail.

The theoretical description is phenomenological in the sense that the kinetic equations do not directly contain information about the groups involved in proton transfer. However, the model does contain geometric, energetic, and kinetic parameters that come from the enzyme structure, the assumptions of the model, and the calculated protonation energies. Thus, in such modeling, the agreement with experiment is a necessary but not sufficient condition, and cannot be taken as a rigorous proof of the model (e.g., that His291 is the pump element of the enzyme). Indeed, any model that is identical to ours in all other resects but with a different pump element located in the vicinity of His291 would kinetically behave in a similar way. In this respect, the kinetic description discussed here is quite general. In the past, many schemes that are built around the idea that the chemical protons electrostatically displace the pumped proton [35,36] have been proposed and could in principle be kinetically described in the way we discuss here.

We find that the His291 model considered here does largely reproduce the kinetics of the membrane potential generation observed in the experiments [17–23].

The plan of the paper is as follows. In the next section, we will specify the kinetic model and describe the relations between the transfer rates and the kinetic restrictions necessary for the pumping to occur. We then discuss the available experimental data and the comparison of theoretical predictions with experiment.

2. The model

The proposed proton-pumping scheme is shown in Fig. 1, and the corresponding four-state model is shown in Fig. 2. The kinetic description is similar to that of our recent work [37] where the flush-photolysis experiments with the CO-bound mixed-valence enzyme [38–40] were analyzed.

The catalytic cycle of the enzyme is rather complicated and involves four electrons and eight protons, see e.g., [25]. Here, we will consider only one step in the cycle, the so-called F → O transition. We believe, however, that a similar kinetic model with somewhat different energetic parameters can be applied to describe all other transitions, including O → E transition, in which the chemical proton is believed to come through the K channel rather than the D channel [31,32]. The four relevant states, which determine the development of the membrane potential, are shown in Fig. 2. These states are: (1) = (a, b) is the state where both OH⁻ in the binuclear catalytic site (BNC), in
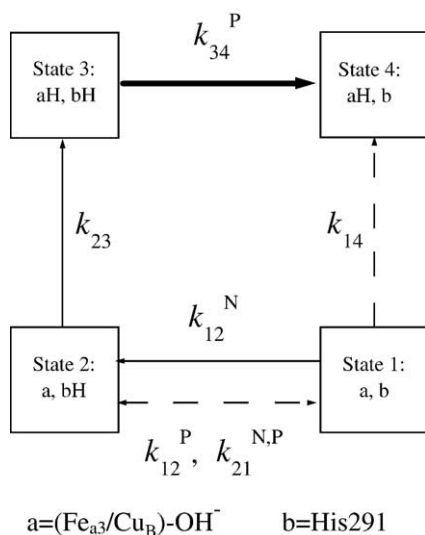
Fig. 2. The four-states model for the proton pump element: (a) the OH^- ligand at the binuclear Fea3–CuB center; (b) His291 (bovine)—the proposed Proton Loading Site (PLS) of the pump. Full lines are proton transfers leading to proton pumping; dashed lines are proton "leaks" reducing the efficiency of proton pumping. The thick line shows rapid expulsion of the proton from PLS to the P-side of the membrane simultaneous with the protonation of the BNC. $k_{12}^{N/P}$ are the rates of protonation of His291 from the negative (N), or positive (P) sides of the membrane. k_{34}^{P} is the rate of deprotonation of His291, with the proton expulsion to the P-side of the membrane.

short we call it group (a), and His291, group (b), are deprotonated; $(2)=(a, bH)$ is the state where only His291 is protonated; $(3)=(aH, bH)$ is the state where both His291 and OH^- in the catalytic site are protonated; and $(4)=(aH, b)$ is the state where His291 is deprotonated, and OH^- is protonated. His291, group b, plays the role of a Proton Loading Site (PLS) of the pump [25,34].

In addition to His291 and OH^- group in the catalytic site, the third important element of the model is Glu242, group (g) for short, the source of protons for both chemistry and pumping (see above remark about the K channel). This group has been shown experimentally to have pK_a greater than 9, and is in the fast protonic equilibrium with the negative side of the membrane, see Fig. 1 [41–44]. Following these experimental data, we assume that reprotonation of Glu242 is a much faster process than other transitions in the system, and, therefore, we do not need to explicitly include various protonation states of this group in our kinetic model. Instead, the effective rates of protonation from the N side of the membrane are proportional to the equilibrium fraction of protonated Glu242, and this dependence can in principle give rise to a pH dependence at high pH of the observed kinetics.

The protons can be uptaken/released from/to the N side and the P side of the membrane. Correspondingly, k_{12}^N in Fig. 2 stands for the rate of protonation of the His291 from the N side of the membrane, i.e., the rate of the Glu242→His291 proton transfer; k_{12}^P denotes the rate of protonation of the His291 from the P side, etc.

The proton transitions are initiated by the fast electron transfer from Cu_A to heme a and then to heme a_3/Cu_B binuclear catalytic site, BNC. According to our model, the

sequence of proton transfer events leading to proton pumping is $(1)→(2)→(3)→(4)$, or $(a, b)→(a, bH)→(aH, bH)→(aH, b)$, with one proton moving from the N side towards the P side of the membrane, and one proton reaching the OH^- group in BNC, and forming water molecule.

3. Kinetic assumptions of the model

One can easily write down the generic kinetic equations for the scheme shown in Fig. 2 and analyze various possibilities that would depend on the energies and rates of individual transitions. We will present a study of the generic case elsewhere, here our goal is to make a connection with experimental data, therefore, we will restrict the discussion to a specific case, which we propose is realized in the enzyme. The assumptions of the model are specified below.

(1) The key assumption of the model is that in the reduced state of BNC (i.e., when the total charge on the metal plus its ligand is +2 for Fea3, and +1 for CuB, see [25]) the rate of proton transfer from Glu242 to His291 is much higher than that to OH^- group in BNC, although the latter group is more favorable energetically. The structural basis for this assumption is discussed in Ref. [25], which results from the computer simulation of behavior of water chains in the catalytic center [27,28]. In the simulation the fully reduced enzyme was used, and an assumption is made that a similar structure of water chains is maintained during the whole cycle of the enzyme. In the notation adopted in Fig. 2, we therefore assume

$$k_{12} \gg k_{14}. \tag{1.1}$$

The degree to which this assumption holds can be related to the efficiency of the pumping. Indeed, if the mechanism of the enzyme is of pure kinetic nature, i.e., there is no switch between the channels for Glu242 to His291, and Glu242 to BNC proton transfers, and these two channels are independent/uncorrelated, then the efficiency of loading of the pump proton onto the pump site His291 is given by the ratio $k_{12}/(k_{12}+k_{14})$. This assumption, and its consequences, will be further discussed later in the paper, when we introduce relevant experimental data.

(2) Next assumption is that protonation of His291 occurs from the N side of the membrane, and not from the P side, although the latter process is energetically more favorable. This kinetic gating can be regulated by specific energy profile of proton-conducting channels [26,34]. Thus, the assumption is

$$k_{12}^N \gg k_{12}^P. \tag{1.2}$$

In the experiments, where Glu242 is mutated, or the D channel is blocked, the residual reduction of oxygen to water by CcO is observed [45] and this is attributed to the supply of protons from the P side of the membrane called "leaking". This process is much slower than the physiological turnover of the enzyme, which is consistent with the above assumption.

(3) Expulsion of the proton from His291 occurs to the P side of the membrane, the opposite side to one from which

His291 was previously protonated. This assumption again is of kinetic nature because the P side has a higher chemical potential than the N side. The basis for this is twofold. First is that Glu242, a group through which the proton can reach the N side, is most likely already re-protonated by the time of the expulsion transition, and therefore will block the back proton transfer. Also, the expulsion is due to repulsion between the chemical proton in BNC and a proton on His291; the geometry of the enzyme is such that the back transfer from His291 is also partially blocked by the chemical proton [25]. The assumption translates into the following:

$$k_{34}^{P} \gg k_{34}^{N}. \tag{1.3}$$

(4) There is one more restriction on k_{34}^{P}, which is not related to the pumping mechanism per se, but follows from the kinetic experimental data. In experiment, only two protonic kinetic phases are observed, see below. Intrinsically, our pumping model has more than two protonic timescales. For example, even when the BNC has become protonated, the other proton can still reside on His291 for a significant period of time, depending on the exit barrier height, before getting expelled to the P side of the membrane. The expulsion process could itself give a separate kinetic phase, in addition to the His291 loading phase and the BNC protonation phase. However, only two phases are resolved experimentally [17–23]. This means that, within the framework of our model, we need to assume that the expulsion of the proton from the PLS shown by thick line in Fig. 2 occurs simultaneously with protonation of the BNC, so that these two kinetic phases actually merge into one single phase. This leads to the kinetic restriction

$$k_{34}^{P} \gg k_{12}, k_{23}. \tag{1.4}$$

Practically speaking, a 10-fold difference between the rates would be sufficient for the described conditions. However, in even less stringent condition would in some cases work too; for example the degree to which condition (1.1) holds depends on how efficient we want the pump to be, see later discussions in the text.

The above assumptions allow maximum simplification of the kinetic scheme shown in Fig. 2, and in practice, results in a sequential irreversible transfer scheme:

$$(1) \rightarrow (2) \rightarrow (3) \rightarrow (4).$$

We will restrict ourselves to this simplified scheme, which directly mimics the observed kinetics of the membrane potential.

Under the above assumptions, the kinetics of the populations, p_1, p_2, p_3, p_4, of the above states is reduced to the following:

$$p_1(t) = e^{-k_{12}t}, \tag{1.5}$$

$$p_2(t) = \frac{k_{12}}{k_{12} - k_{23}} \left(e^{-k_{23}t} - e^{-k_{12}t} \right). \tag{1.6}$$

The population p_3 is close to zero due to the high rate k_{34}^{P} (assumption 4), hence the normalization condition for populations is reduced to

$$p_1 + p_2 + p_4 = 1, \qquad p_3 = 0, \tag{1.7}$$

from which p_4 can be determined. The populations of these states allow one to calculate the membrane potential.

The potential is calculated as follows. The total membrane potential is due to electron transfer from Cu_A to the BNC and due to transport of protons induced by the electron transfer.

The electron transport involves two transfers: Cu_A to heme a, and heme a to heme a_3/BNC, see Fig. 1. The position of heme a and BNC is such that from heme a to BNC electron moves essentially parallel to the membrane, therefore electronic transition from heme a to BNC does not contribute to the potential. Next, following the discussion in Refs. [22,23] we assume that the injection of an electron into the system results in less than 100% transfer of the electron to BNC. The fraction of the transferred electron to BNC is called β. The rest, $(1 - \beta)$, is believed to remain on Cu_A until protons are transferred to BNC, or a region near BNC, and stabilize the electronic acceptor. This is presumably due to similar redox potentials of Cu_A and heme a, and equilibration of an electron between the two sites, which occurs faster than the subsequent electron transfer between heme a and heme a3 that is coupled to and limited by a slow proton transfer to BNC.

The pure electronic transition from Cu_A to heme a occurs on the fastest time-scale (order of ten microseconds) and, compared with much slower protonic phases (order of hundred microseconds to milliseconds), can be considered as instantaneous. The protonic contribution to the membrane potential involves charge transfer to PLS (His291) from the N-side, one proton transfer to BNC (OH^-) from the N-side, and the expulsion of the proton from PLS to the positive side of the membrane, which occurs simultaneously in our model with protonation of BNC.

Given the above assumptions, the membrane potential can be written as follows (see Fig. 1):

$$V_{tot}(t) = V_{el}\beta + p_2[V_b + V_{el}(1 - \beta)]$$
$$+ p_4[V_a + V_0 + V_{el}(1 - \beta)]. \tag{1.8}$$

The first term $V_{el}\beta$ describes the pure electronic contribution; the second term corresponds to a proton transfer to PLS, which generates potential V_b and also pulls the additional fraction $(1 - \beta)$ of electrons to the BNC, which generates potential $V_{el}(1 - \beta)$; the third term corresponds to a proton transfer to BNC with simultaneous expulsion of the proton from PLS to the positive side of the membrane (thick line in Fig. 2). When the last state (4) is produced, the proton in BNC generates potential V_a, one proton appears on the positive side of the membrane, which corresponds to a total crossing of the whole membrane and generation of the potential V_0, and in addition, each proton passing through the membrane also pulled the $(1 - \beta)$ fraction of electrons, hence generating an additional membrane potential $V_{el}(1 - \beta)$.

The potentials V_{el}, V_a, V_b, V_0, can be correlated with the geometry of the system. If we assume a homogeneous dielectric membrane, each of the potentials is proportional to the depth of the position of the corresponding site in the membrane. Thus, V_0, is proportional to the total thickness of the membrane, L_0, V_{el} is proportional the distance L_{el} from the P side to heme a, as shown in Fig. 1, etc. Since in the experiment only *relative* potentials can be determined, we will measure all distances relative to the total thickness of the membrane L_0, which is assigned the value $L_0 = 1$.

(The assumption of homogeneous dielectric throughout the protein is probably not very accurate, primarily because of the internal water in the enzyme [3], in particular "above" the hemes area, see Fig. 1. In the Appendix of this paper we show how the results discussed below are changed, if we assume a simple model which includes dielectric inhomogeneity of the protein. The change is found to be relatively small therefore these results are summarized in Appendix A.)

Using the time-dependent populations from Eqs. (1.5)–(1.7), one can calculate the time development of the membrane potential, which can be directly compared with experimental measurements.

4. Comparison with experiment

In the experiment, three kinetic phases in the development of the membrane potential are observed: one electronic (order of ten microseconds) and two protonic phases, fast and slow (order from hundreds of microseconds to few milliseconds). The two protonic phases are described as follows:

$$V_{prot}^{exp}(t) = V_f\left(1 - e^{-k_f t}\right) + V_s\left(1 - e^{-k_s t}\right), \quad (1.9)$$

where k_f and k_s are the rates, and V_f and V_s are the amplitudes of the fast and slow protonic phases. According to our model, we associate the fast process with a proton transfer to His291 (PLS), with the rate $k_f = k_{12}$, and the slow process with a proton transfer to OH^- group in BNC, with rate $k_s = k_{23}$. Comparing the above experimental expression with the theoretical one in Eq. (1.8), we find the following correspondence:

$$V_f = V_b + V_{el}(1 - \beta) - \frac{k_{23}}{k_{12} - k_{23}}(V_a + V_0 - V_b), \quad (1.10)$$

$$V_s = \frac{k_{12}}{k_{12} - k_{23}}(V_a + V_0 - V_b). \quad (1.11)$$

As one can see, the observed amplitudes of the fast and slow kinetic phases are not directly related to the geometry of the system (i.e., to potentials V_{el}, V_a, V_b, V_0). It is, however, the case when the timescales of the fast and slow phases are indeed significantly different, say by one order of magnitude. If $k_{12} \gg k_{23}$, then the fast component would correspond to potential $V_b + V_{el}(1 - \beta)$ and the slow one to $V_a + (V_0 - V_b)$, as expected. The experimental rates of the fast and slow phases are not too much different, which leads to a partial overlap of the fast and slow kinetics, and the

modified kinetic relations above. We find this difference to be crucial for the correct interpretation of the experimental data, as shown below.

The comparison with experiment will be done by assigning the values of k_{12} and k_{23} to the experimental values of the fast and slow protonic phases, $k_{12} = k_f$, $k_{23} = k_s$, and comparing the calculated value of the ratio of the amplitudes (V_f/V_s) with that observed in experiment.

The geometric parameters L_{el}, L_a, L_b, L_0 needed to calculate potentials V_{el}, V_a, V_b, V_0 were estimated from the available crystal structures. The distances are about the same in bacterial and bovine enzymes. For the bovine enzyme [3], the relative distances are shown in Fig. 1, together with the experimental values of β for different enzymes. The most critical data here is for the position of the Proton Loading Site (PLS). The identity of this group is not known with certainty. Thus, our proposal that His291 is the PLS of the pump is reflected in the present model only in the position of this group inside the membrane.

Below, we discuss the experimental data reported recently for different systems and for several mutants, and compare these data with the predictions of the model.

4.1. R. sphaeroides

For a wild type CcO from *R. sphaeroides*, Konstantinov et al. [19] observed two protonic phases in the kinetics of the membrane potential when a single electron injected into the system drives it from state F to state O. The experimental kinetics is represented as discussed above, Eq. (1.9), and the observed rates and amplitudes are as follows: $k_f = (0.4 \text{ ms})^{-1}$, $k_s = (1.5 \text{ ms})^{-1}$, and $(V_f/V_s) = 0.4$ for pH 8. Notice that the rates of the fast and slow phases are not much different.

Using the geometrical parameters from Fig. 1 and the experimental value of $\beta = 0.75$ for the bacterial enzyme [23], we obtain $L_{el} = 0.31$ (which is close to the empirical value of 0.32 given in paper [23] for mitochondrial CcO), and for the ratio of the amplitudes we find $(V_f/V_s) = 0.45$ in agreement with experiment [19].

It is worthwhile to demonstrate here the significant difference between the "intrinsic" amplitudes of the potential generated in elementary events of charge transfers (i.e., potentials $\bar{V}_f = V_b + V_{el}(1 - \beta)$ and $\bar{V}_s = V_a + (V_0 - V_b)$) and the "apparent" amplitudes observed in experiment V_f and V_s, as predicted by our theoretical expressions, Eqs. (1.10) and (1.11). For instance, for the bacterial enzyme (data by Konstantinov et al. [19]), where $k_s/k_f = 0.27$, we would calculate $(\bar{V}_f/\bar{V}_s) = (V_b + V_{el}(1 - \beta))/(V_a + (V_0 - V_b)) = 0.98$, which is more than twice the experimental value $(V_f/V_s) = 0.4$. In general, the apparent amplitudes are functions of the rates because of the partial overlap of the two phases. Still, the sum of the apparent amplitudes is equal to the sum of the intrinsic amplitudes, as follows from Eqs. (1.10) and (1.11).

4.2. P. denitrificans

Ruitenberg et al. [20,21] have reported the rates and amplitudes for the F to O transition in the bacterial enzyme

from *P. denitrificans* similar to those of Konstantinnov et al. [19] for the *R. sphaeroides* . In the latest work of this group [21], the rates and amplitudes for *P. denitrificans* were reported to be $(k_f = 0.27 \text{ ms})^{-1}$, $k_s = (1.5 \text{ ms})^{-1}$, and $(V_f / V_s) = 0.5$. Inserting the experimental rates into Eqs. (1.10) and (1.11), we obtain $(V_f / V_s) = 0.62$, which again is close to the experimental value.

4.3. Bovine heart CcO

Several measurements have been performed on the enzyme from bovine heart. Zaslavsky et al. [18] have reported three kinetic phases in time-resolved spectroscopic measurements of the kinetics of the F to O transition generated by electron injection into the F state of the enzyme. The phases were assigned to be one electronic and two protonic ones. The observed rates and amplitudes of the protonic phases are: $k_f = (1.1 \text{ ms})^{-1}$, $k_s = (4.9 \text{ ms})^{-1}$, and $(V_f / V_s) = 0.4$. Our calculations with these rates give $(V_f / V_s) = 0.6$. Here, for bovine enzyme we used $\beta = 0.5$ [22]. (If we use $\beta = 0.75$, our calculations give $(V_f / V_s) = 0.5$). The difference with the experimental value could be viewed as insignificant considering a large experimental error reported in Table 1 of Ref. [18], and that the method does not directly correspond to potential measurements.

For the membrane potential generated by a bovine enzyme in the F to O transition, Siletsky et al. [17] (see Table 2 in their paper) report the following values: $k_f = (1.2 \text{ ms})^{-1}$, $k_s = (4.5 \text{ ms})^{-1}$, and $(V_f / V_s) = 0.33$, whereas our theoretical value is $(V_f / V_s) = 0.51$, for $\beta = 0.5$, and $(V_f / V_s) = 0.45$ for $\beta = 0.75$.

When comparing experimental and theoretical values, one should consider, among other factors, the uncertainty in the interpretation of the experimental data obtained with different measurement methods [22].

4.4. R. sphaeroides mutants

4.4.1. E286Q

In frames of our model, the experimental results of Gennis, Konstantinov and co-workers [17,19] on the mutants of *R. sphaeroides* enzyme can be rationalized. In the E286Q (E242 in bovine) enzyme, the two millisecond phases (presumably both protonic phases) in the potential kinetics are completely absent. As suggested by Konstantinnov et al. [19], since it is unclear whether E286Q forms the ferryl-oxo state upon addition of H_2O_2 in their experiment, the above result could be a consequence of E286Q simply not being able to generate the ferryl-oxo form under their experimental conditions. However, if E286Q does generate the ferryl-oxo form, then our model, as any model in which E286 is a passing point for both pumped and chemical protons in the F to O transition, would explain the observed results as the absence of the proton donor E286 (E242 in bovine, our group g) for both of these phases.

4.4.2. D132N

In the D132N mutant [19] the proton donor E286 (bovine E242, group g) is present but its re-protonation from the N side of the membrane is blocked. D132 is the entrance of the D channel through which protons are supplied from the N side of the membrane. Our model suggests that in this mutant the proton still can move from E286 to PLS (bacterial equivalent of His291), but there will be no second, chemical proton to complete the cycle of proton pumping, and only one (fast) phase should be observed. The amplitude of this phase is directly related to the position of the PLS site and is proportional to the distance between PLS site and E286; thus, this amplitude is predicted to be $\tilde{V}_f = (V_b - V_g) = (L_b - L_g) = 0.25$. An additional contribution to this phase may come from the fraction of the electron remaining on Cu_A, $V_{el}(1-\beta) = 0.16$. We counted both of these contributions.

In agreement with this picture, in the experiment [19], in place of the two protonic phases, in the D132N mutant only a single phase is observed, which is called intermediate phase in Ref. [19]. This phase was argued to be equivalent to and to be compared with the fast protonic phase of the WT enzyme. The amplitude of this phase is observed to be 2–3 times smaller than that of the fast phase of the WT enzyme. Our model gives a factor of 1.7 for this ratio.

The small difference with the experiment might be due to several factors, including unaccounted conformational changes in the mutant enzyme with respect to WT. Such changes are indeed observed (see, e.g., [14]), but would be difficult to describe quantitatively in the kinetics. The conformational changes may be also responsible for the inhibition of both protonic phases of the F to O transition in the equivalent D124N mutant of *P. denitrificans* [21]. However, the more likely factor that could affect the difference between the calculated and observed amplitudes is the incomplete conversion of the mutant enzyme to the ferryl-oxo state F by the H_2O_2 treatment [17] in the experiment. Qualitatively, this effect results in the lower amplitudes in the mutant enzyme compared to WT, where the conversion is expected to be complete. Therefore, this effect should increase the ratio of the amplitudes of the fast phases of WT and the mutant, and could in principle be responsible for the difference between the theoretical factor 1.7 and experimentally observed factors 2–3.

4.4.3. N139D

The N139D mutant does not pump protons, while the turnover rate, i.e., the rate of delivery of chemical protons to the catalytic center, is increased by a factor of 2–3 [17,46]. In the N139D mutant the rates of proton transfer along the D channel, and in particular between E286 (E242 in bovine, our group g) and PLS (His291 in bovine, group b), are presumably modified. This is likely the result of some subtle structural changes in the D channel, in particular in the arrangement of internal water molecules in the D channel of the protein. In terms of our model, in the mutant, the rate of proton transfer from E286 to PLS (group a) k_{12} is presumably decreased, and/or the rate of proton delivery to the binuclear center k_{14} is increased (this assumption is supported by the observed increased turnover rate of the enzyme), so that the key assumption of the kinetic model, $k_{12} \gg k_{14}$ is no longer satisfied. That means that in the mutant the proton loading to PLS, which should occur before the chemical proton is

delivered to the catalytic center, does not happen, and therefore no pumping should be observed.

According to our model, in this case the only electrogenic process to occur is proton transfer from the negative side of the membrane directly to the catalytic center, BNC, bypassing the proton loading and pumping steps. Only a single kinetic phase is predicted to be observed with the amplitude $\tilde{V}_s = V_a + V_{el}(1-\beta) = 0.8$, which should correspond to the slow kinetic phase observed in the WT enzyme.

In the experiments with the N139D mutant reported recently by Siletsky et al. [17] indeed only a single protonic phase is observed. The data reported in Table 2 of their paper show that the amplitude of the single protonic phase in the mutant, corrected for the incompleteness of the reaction with hydrogen peroxide, is decreased by a factor of 1.3 with respect to the amplitude of the slow protonic phase in the WT enzyme. Our model gives a corresponding value of 1.6. The interpretation given in Ref. [17] is practically identical to the one that follows from our model.

The degree to which one of the key assumptions of the model $k_{12} \gg k_{14}$ holds (i.e., the rate of proton transfer from Glu242 to His291 is higher than that from Glu242 to OH$^-$ in BNC) can be related to the efficiency of the pumping. Indeed, if the mechanism of the enzyme is of pure kinetic nature, i.e., there is no switch between the channels for Glu242 to His291, and Glu242 and BNC proton transfers, and these two channels are independent/uncorrelated, then the efficiency of loading of the pump proton onto the pump site His291 is given by the ratio $k_{12}/(k_{12} + k_{14})$. The rate k_{14} on the other hand, cannot be slower than k_{23}, the rate of Glu242 to BNC proton transfer with His291 protonated (i.e., after the loading), see Fig. 2. In the simplest scenario, the rates k_{14} and k_{23} are simply the same, because of the likely bottleneck of Glu242 to BNC proton transfer. As we discussed earlier in the text, the actual rates that we identify in the experiments as fast and slow correspond to k_{12} and k_{23}, respectively, and are different by roughly factor of 4 to 5; thus the assumption of pure kinetic gating also means the efficiency of the pump should be expected to be at maximum 0.8H+ per electron. Under these circumstances, for the proton pump working according to our model with higher efficiency, some kind of a switch would be required between Glu242 to His291 and Glu242 to BNC channels.

4.5. Experiments with fully reduced enzyme

Recently, Wikström and co-workers have reported experimental measurements of the membrane potential generated by both bovine and bacterial CcO during the reaction of the fully reduced enzyme with oxygen [22,23]. The reaction in this case proceeds via series of spectroscopically resolved steps: R→A→P→F→O. An additional injection of electrons into the enzyme can drive the reaction further, O→E, and finally E→R. The kinetic data for both the F to O and O to E transitions have been discussed.

The O to E transition is different from F to O in that the chemical proton in the O to E transition is delivered to the catalytic center via the K channel instead of the "usual" D channel [31,32], as in the F to O transition. As far as the

mechanism of pumping is concerned, however, this difference, according to our model, is insignificant. Indeed, as long as the rate of proton loading of PLS from the negative side of the membrane, k_{12}, is greater than the rate of protonation of the catalytic center, k_{23}, the pumping should work in qualitatively the same way. Thus, in the O to E transition, we can formally interpret k_{23} as the rate of proton transfer to BNC via the K channel.

We fist discuss an earlier work from Wikström's group, in which a fully reduced enzyme (bovine CcO) is reacted with oxygen and the membrane potential is measured [22]. The reaction proceeds via the R→A→P→F→O transitions. With no a priori assumption made on the nature of the electrogenic steps, the kinetics of the membrane potential was fit by a general multi-exponential expression

$$V_{exp}(t) = \sum_{n=R,A,P,F} C_n F_n(t), \qquad (1.12)$$

where $F_R = 1 - p_R$, $F_A = F_R - p_A$, $F_P = F_A - p_P$, etc., and p_n are populations calculated in a five-step sequential reaction model, and C_n are empirical coefficients [22]. We will apply our model for the last transition F→O, and will use the other empirical parameters as determined by empirical fit by Wikström and co-workers. We therefore will write the calculated potential in the form:

$$V_{calc}(t) = V_{exp}^{R \to F}(t) + C V_{theor}^{F \to O}(t) \qquad (1.13)$$

where $V_{exp}^{R \to F}$ is the part of the fitting expression (1.12) with $n = R$, A, P, taken with parameters (the amplitudes and rates of individual transitions) of Ref. [22], $V_{theor}^{F \to O}$ is the calculated potential using our model, Eq. (1.8), and C is the scaling factor.

The population p_1, which was previously calculated as Eq. (1.5), now has to be modified to account for the exchange with the previous state P,

$$\dot{p}_1 = -k_{12} p_1 + k_{P1} p_P, \qquad (1.14)$$

where both k_{P1} and population of the P state were taken from Ref. [22]. The scaling factor C is the potential generated upon transfer of one charge unit across the membrane. According to the data of Ref. [22] the potential of 2.25 mV is generated when electron is transferred from heme a to Cu_A in the backflow reaction. Therefore, the numerical value of C is calculated to be $C = -2.25$ mv/L_{el}. The values of $\beta = 0.5$ and $L_{el} = 0.31$ for bovine heart CcO were taken from [22].

In Fig. 3, the potential calculated as described above is shown together with the experimental data. Two sets of the rate parameters have been explored. The first set included no major leaks (see the dashed lines in Fig. 2.) The result of the calculation is shown by solid line 1 in Fig. 3. We find that a better agreement with experiment can be achieved if one assumes a non-perfect function of the pump, and allows the direct protonation of BNC to compete with the loading of PLS, i.e., to assume a non-zero rate k_{14}, in terms of the scheme in Fig. 2. This modification improves the comparison with experiment, as shown by curve 2 in Fig. 3, however, it also results in the loss of the pumping efficiency. For the
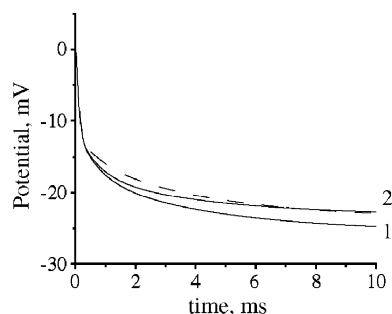
Fig. 3. The membrane potential generated by CcO during the reaction of the fully reduced enzyme with oxygen. Dashed line is the experimental curve from Fig. 2 of Ref. [22]; solid lines are theoretical curves, see text (curve 1, pumping efficiency 100%, curve 2, pumping efficiency 70%).

parameters used to calculate curve 2, the efficiency was about 70%.

In a more recent work, Bloch et al. [23] have reported the kinetics of the O→E transition upon a single electron injection in *P. denitrificans* enzyme. The O state was prepared by reacting the fully reduced enzyme with oxygen. The amplitudes of all kinetic phases, one electronic and two protonic, are well resolved as in the F→O transition. When comparing the model with experiment, in addition to the ratio of the amplitudes of the protonic phases discussed above, one more important test of the model is to compare with experiment the ratio of the amplitude of the electronic phase to the amplitudes of both protonic phases.

We use the following data for our calculations: $k_f = (0.2$ ms$)^{-1}$, $k_s = (1.4$ ms$)^{-1}$, and $\beta = 0.75$ are taken from experimental data, $L_{el} = 0.32$, $L_a = 0.69$, $L_b = 0.8$ are from the crystal structure geometry. Using Eqs. (1.10) and (1.11), from our model we find for the ratios of protonic and electronic phases $(V_{slow}^{prot}/V^{elec}) = 4.6$ and $(V_{fast}^{prot}/V^{elec}) = 3.2$, while the authors of Ref. [23] have reported that the fast and slow protonic phases have about the same amplitude in their experiment, which agrees with our prediction.

5. Conclusions

Two most important conclusions of this work are as follows:

(1) The kinetic overlap of the "fast" and "slow" protonic phases results in a specific non-trivial relation between the apparent amplitudes obtained in experiment and geometric parameters of the model, Eqs. (1.10) and (1.11), which is important to use for a correct interpretation of experimental results on the kinetics of the membrane potential generated by cytochrome *c* oxidase.

(2) A reasonable agreement with five different experiments with both bovine and two bacterial enzymes, and three different mutants, provides a support for the proposed kinetic model of the CcO pump. The elements of this model are: the two chains of water molecules in the cavity around the binuclear catalytic center [16,27,28], the kinetic gating of the pumped and chemical protons [25], and a proposal that His291 (in bovine notation) is the Proton Loading Site of the pump [24].

Yet, the agreement is not a proof of the model, because the identity of the PLS group is not explicitly present in the phenomenological kinetic description of the present analysis. We can conclude with greater confidence, however, on the basis of the location of PLS, which is an explicit parameter of the model, that the PLS should be located in the vicinity of His291, if it is not His291 itself.

Due to the phenomenological nature, the degree of applicability of the developed kinetic scheme is broader that just the His291 model discussed here. In fact, any generic model in which the pumped protons are displaced by the incoming chemical protons can be described with our theory.

(3) The assumption of pure kinetic gating adopted here means the efficiency of the pump should be expected to be at maximum 0.8H+ per electron. Under these circumstances, for the proton pump working according to our model with higher efficiency, some kind of a switch would be required between Glu242 to His291 and Glu242 to BNC channels.

Thus if the efficiency of CcO is indeed higher than say 80%, the analysis suggests that there is a some kind of a switch that regulates the proton transfers between Glu242 and His291, and Glu242 and OH⁻ in BNC. One possibility was discussed recently in Ref. [16]. On the other hand, such a switch obviously would require some subtle molecular mechanism, which would be a non-trivial task for the molecular evolution to accomplish, all just to improve the efficiency of the pump from 80 to 100%. The situation obviously is not very clear, and requires further studies.

Appendix A

Here, we show how the results discussed in the paper are changed if the inhomogeneity of the protein is taken into account. We assume that the dielectric constant of the protein above His291, see Fig. 1, is increased by a factor ε, compared with that below His291, so that the effective length of proton transfer from His291 to the P-side of the protein is decreased by a factor of ε. The increased dielectric constant qualitatively accounts for the water cluster located in that region of the protein. At the same time, we assume that the electron transfer path Cu$_A$ to heme a runs through the unchanged low dielectric medium (this contribution is minor, in any case). In this case the apparent fast

and slow protonic amplitudes are given by (cf. Eqs (1.10), (1.11)):

$$V_f = V_b + V_{el}(1-\beta) - \frac{k_{23}}{k_{12}-k_{23}}\left(V_a + \frac{V_0-V_b}{\varepsilon}\right) \quad (A1)$$

$$V_s = \frac{k_{12}}{k_{12}-k_{23}}\left(V_a + \frac{V_0-V_b}{\varepsilon}\right) \quad (A2)$$

The change of the results are summarized in the Table below. First column for convenience reproduces results discussed in the text. The last two columns correspond to experimental data, and reference from which the data were taken. The data should be considered only as showing a qualitative trend, because the actual dielectric inhomogeneity of the protein is difficult to quantify.

Table A1. Influence of the high dielectric constant above His291 region. The data are shown in the order discussed in the main text.

	$\varepsilon=1$	$\varepsilon=4$	$\varepsilon=20$	exp	ref
V_f/V_s	0.45	0.58	0.63	0.4	[19]
V_f/V_s	0.62	0.77	0.82	0.5	[21]
V_f/V_s	0.60 ($\beta=0.5$)	0.75	0.80	0.4	[18]
V_f/V_s	0.53 ($\beta=0.75$)	0.67	0.72		
V_f/V_s	0.51 ($\beta=0.5$)	0.66	0.70	0.33	[17]
V_f/V_s	0.45 ($\beta=0.75$)	0.58	0.63		
$V_f(WT)/V_f(D132N)$	1.70	1.86	1.90	2–3	[19]
$V_s(WT)/\tilde{V}_s(N139D)$	1.6	1.31	1.25	1.3	[17]
V_{slow}^{prot}/V^{elec}	4.6	3.9	3.7	"about the	[23]
V_{slow}^{prot}/V^{elec}	3.2	3.3	3.3	same"	

References

[1] S. Iwata, C. Ostermeier, B. Ludwig, H. Michel, Structure at 2.8 Å resolution of cytochrome *c* oxidase from *Paracoccus denitrificans*, Nature 376 (1995) 660–669.
[2] T. Tsukihara, H. Aoyama, E. Yamashita, T. Tomizaki, H. Yamaguchi, K. Shinzawa-Itoh, R. Nakashima, R. Yaono, S. Yoshikawa, Structure of metal sites of oxidized bovine heart cytochrome *c* oxidase at 2.8 Å, Science 269 (1995) 1069–1074.
[3] S. Yoshikawa, K. Shinzawa-Itoh, R. Nakashima, R. Yaono, E. Yamashita, N. Inoue, M. Yao, M.J. Fei, C.P. Libeu, T. Mizushima, H. Yamaguchi, T. Tomizaki, T. Tsukihara, Redox-coupled structural changes in bovine heart cytochrome *c* oxidase, Science 280 (1998) 1723–1729.
[4] M. Wikstrom, Proton pump coupled to cytochrome *c* oxidase in mitochondria, Nature 266 (1977) 271.
[5] R.B. Gennis, How does cytochrome oxidase pump protons? Proc. Natl. Acad. Sci. U. S. A. 95 (1998) 12747.
[6] H. Michel, Cytochrome *c* oxidase: catalytic cycle and mechanism of proton pumping—A discussion, Biochemistry 38 (1999) 15129–15140.
[7] H. Michel, Proton pumping by cytochrome *c* oxidase, Nature 402 (1999) 602–603.
[8] M. Wikström, Proton translocation by cytochrome *c* oxidase: a rejoinder to recent criticism, Biochemistry 39 (2000) 3515–3519.
[9] S.M. Musser, S.I. Chan, Understanding the cytochrome *c* oxidase proton pump: the thermodynamics of redox linkage, Biophys. J. 68 (1995) 2543–2555.
[10] S. Riistama, G. Hummer, A. Puustinen, B.R. Dyer, W.H. Woodruff, M. Wikstrom, Bound water in proton translocation mechanism of the heme-copper oxidase, FEBBS Lett. 414 (1997) 275–280.
[11] H. Michel, The mechanism of proton pumping by cytochrome *c* oxidase, Proc. Natl. Acad. Sci. U. S. A. 95 (1998) 12819–12824.
[12] T.K. Das, C.M. Gomes, M. Teixeira, D.L. Rousseau, Redox-linked transient deprotonation at the binuclear site in the aa3-type quinol oxidase from *Acidianus ambivalens*: implications for proton translocation, Proc. Natl. Acad. Sci. U. S. A. 96 (1999) 9591–9596.
[13] M. Wikström, Mechanism of proton translocation by cytochrome *c* oxidase: a new four-stroke histidine cycle, Biochim. Biophys. Acta 1458 (2000) 188–198.
[14] P. Brzezinski, G. Larsson, Redox-driven proton pumping by heme-copper oxidases, Biochim. Biophys. Acta 1605 (2003) 1–13.
[15] T. Tsukihara, K. Shimokata, Y. Katayama, H. Shimada, K. Muramoto, H. Aoyama, M. Mochizuki, K. Shinzawa-Itoh, E. Yamashita, M. Yao, Y. Ishimura, S. Yoshikawa, The low-spin heme of cytochrome *c* oxidase as the driving element of the proton-pumping process, Proc. Natl. Acad. Sci. 100 (2003) 15304–15309.
[16] M. Wikstrom, M.I. Verkhovsky, G. Hummer, Water-gated mechanism of proton translocation by cytochrome *c* oxidase, Biochim Biophys Acta 1604 (2003) 61–65.
[17] S.A. Siletsky, A.S. Pawate, K. Weiss, R.B. Gennis, A.A. Konstantinov, Transmembrane charge separation during the ferryl-oxo→oxidized transition in a nonpumping mutant of cytochrome *c* oxidase, J. Biol. Chem. 279 (2004) 52558–52565.
[18] D. Zaslavsky, A.D. Kaulen, I.A. Smirnova, T. Vygodina, A.A. Konstantinov, Flash-induced membrane potential generation by cytochrome *c* oxidase, FEBS Lett. 336 (1993) 389–393.
[19] A.A. Konstantinnov, S. Siletsky, D. Mitchell, A. Kaulen, R.B. Gennis, The Role of the two proton input channels in cytochrome *c* oxidase from *Rhodobacter sphaeroides* probed by the effects of site-directed mutations on time-resolved electrogenic intraprotein proton transfer, Proc. Natl. Acad. Sci. U. S. A. 94 (1997) 9085–9090.
[20] M. Ruitenberg, A. Kannt, E. Bamberg, B. Ludwig, H. Michel, K. Fendler, Single-electron reduction of the oxidized state is coupled to proton uptake via the k pathway in paracoccus denitrificans cytochrome *c* oxidase, Proc. Natl. Acad. Sci. U. S. A. 97 (2000) 4632–4636.
[21] M. Ruitenberg, A. Kannt, E. Bamberg, K. Fendler, H. Michel, Reduction of cytochrome *c* oxidase by a second electron leads to proton translocation, Nature 417 (2002) 99–102.
[22] A. Jasaitis, M.I. Verkhovsky, J.E. Morgan, M.L. Verkhovskaya, M. Wikstrom, Assignment and charge translocation stoichiometries of the major electrogenic phases in the region of cytochrome *c* oxidase with dioxygen, Biochemistry 38 (1999) 2697–2706.
[23] D. Bloch, I. Belevich, A. Jasaitis, C. Ribacka, A. Puustinen, M.I. Verkhovsky, M. Wikström, The catalytic cycle of cytochrome *c* oxidase is not the sum of its two halves, Proc. Natl. Acad. Sci. U. S. A. 101 (2004) 529–533.
[24] D.M. Popovic, A.A. Stuchebrukhov, Electrostatic study of the proton pumping mechanism in cytochrome *c* oxidase, J. Am. Chem. Soc. 126 (2004) 1858–1871.
[25] D.M. Popovic, A.A. Stuchebrokhov, Proton pumping mechanism and catalytic cycle of cytochrome *c* oxidase: Coulomb pump model with kinetic gating, FEBS Lett. 566 (2004) 126–130.
[26] A.A. Stuchebrukhov, Electron transfer coupled to proton translocation. Proton pumps, cytochrome oxidase, and biological energy transduction, J. Theor. Comp. Chem. 2 (2003) 91.
[27] X. Zheng, D.M. Medvedev, J. Swanson, A.A. Stuchebrukhov, Computer simulations of internal water in cytochrome *c* oxidase, Biochim. Biophys. Acta 1557 (2003) 99–106.
[28] M. Tashiro, A.A. Stuchebrukhov, Thermodynamic properties of internal water molecules in the hydrophobic cavity around the catalytic center of cytochrome *c* oxidase, J. Phys. Chem., B 109 (2005) 1015–1022.
[29] M.L. Verkhovskaya, A. Garcia-Horsman, A. Puustinen, J.-L. Rigaud, J.E. Morgan, M.I. Verkhovsky, M. Wikström, Glutamic acid 286 in subunit I of cytochrome bo3 is involved in proton translocation, Proc. Natl. Acad. Sci. U. S. A. 94 (1997) 10128–10131.
[30] P. Adelroth, M.S. Ek, D.M. Mitchell, R.B. Gennis, P. Brzezinski, Glutamate 286 in cytochrome aa3 from *Rhodobacter sphaeroides* is

involved in proton uptake during the reaction of the fully-reduced enzyme with dioxygen, Biochemistry 36 (1997) 13824–13829.

[31] M. Wikstrom, A. Jasaitis, C. Backgren, A. Puustinen, M.I. Verkhovsky, The role of the D- and K-pathways of proton transfer in the function of the haem-copper oxidases, Biochim. Biophys. Acta 1459 (2000) 514–520.

[32] D. Zaslavsky, R.B. Gennis, Proton pumping by cytochrome oxidase: progress, problems and postulates, Biochim. Biophys. Acta 1458 (2000) 164–179.

[33] D.M. Popovic, J. Quenneville, A.A. Stuchebrukhov, DFT/Electrostatic calculations of pK_a values in cytochrome *c* oxidase, J. Phys. Chem., B 109 (2005) 3616–3626.

[34] D.M. Popovic, A.A. Stuchebrukhov, Proton exit channels in cytochrome *c* oxidase, J. Phys. Chem., B 109 (2005) 1999–2006.

[35] M. Wikstrom, A. Bogachev, M. Finel, J.E. Morgan, A. Puustinen, M. Raitio, M.L. Verkhovskaya, M.I. Verkhovsky, Mechanism of proton translocation by respiratory oxidases. The histidine cycle, Biochim. Biophys. Acta 1187 (1994) 106–111.

[36] P.R. Rich, Towards an understanding of the chemistry of oxygen reduction and proton translocation in the iron-copper respiratory oxidases, Aust. J. Plant Physiol. 22 (1995) 479–486.

[37] A.I. Kotelnikov, D.M. Medevedev, E.S. Medvedev, A.A. Stuchebrukhov, Kinetic treatment of coupled electron and proton transfer in flash-photolysis experiments on carbon monoxide-inhibited mixed-valence cytochrome *c* oxidase, J. Phys. Chem., B 105 (2001) 5789–5796.

[38] S. Hallen, P. Brzezinski, B.G. Malmstrom, Internal electron transfer in cytochrome *c* oxidase is coupled to the protonation of a group close to the bimetallic site, Biochemistry 33 (1994) 1467.

[39] P. Adelroth, P. Brzezinski, B.G. Malmstrom, Internal electron transfer in cytochrome *c* oxidase from *Rhodobacter sphaeroides*, Biochemistry 34 (1995) 2844.

[40] P. Adelroth, H. Sigurdson, S. Hallen, P. Brzezinski, Kinetic coupling between electron and proton transfer in cytochrome *c* oxidase: simultaneous measurements of conductance and absorbance changes, Proc. Natl. Acad. Sci. U. S. A. 93 (1996) 12292.

[41] A. Namslauer, A. Aagaad, A. Katsonouri, P. Brzezinski, Intramolecular proton-transfer reactions in a membrane-bound proton pump: the effect of Ph on the peroxy to 'ferryl transition in cytochrome *c* oxidase, Biochemistry 42 (2003) 1488–1498.

[42] A. Puustinen, J.A. Bailey, R.B. Dyer, S.L. Mecklensburg, M. Wikstrom, W.H. Woodruff, Fourier transform infrared evidence for connectivity between CuB and glutamic acid 286 in cytochrome bo3 from *Escherichia coli*, Biochemistry 36 (1997) 13195–13200.

[43] M. Karpefors, P. Adelroth, P. Brzezinski, The onset of the deuterium isotope effect in cytochrome *c* oxidase, Biochemistry 39 (2000) 5045–5050.

[44] M. Karpefors, P. Adelroth, P. Brzezinski, Localized control of proton transfer through the d-pathway in cytochrome *c* oxidase: application of the proton-inventory technique, Biochemistry 39 (2000) 6850–6856.

[45] D.A. Mills, S. Ferguson-Miller, Proton uptake and release in cytochrome *c* oxidase: separate pathways in time and space, Biochim. Biophys. Acta 1365 (1998) 46–52.

[46] A. Pawate, J.E. Morgan, A. Namslauer, D. Mills, P. Brzezinski, S. Ferguson-Miller, R. Gennis, N139D mutant lacs pumping but has accelerated turnover, Biochemistry 41 (2002) 13417–13423.